THE ASTROPHYSICAL JOURNAL, 465:2–13, 1996 July 1

UNIVERSALITY OF THE NETWORK AND BUBBLE TOPOLOGY IN COSMOLOGICAL GRAVITATIONAL SIMULATIONS

CAPP YESS AND SERGEI F. SHANDARIN
University of Kansas, Lawrence, KS 66045
Received 1995 September 5; accepted 1996 January 12

ABSTRACT

Using percolation statistics we, for the first time, demonstrate the *universal* character of a *network* pattern in the real-space, mass distributions resulting from nonlinear gravitational instability of initial Gaussian fluctuations. Percolation analysis of five stages of the nonlinear evolution of five power-law models [$P(k) \propto k^n$ with $n = +3, +1, 0, -1$, and -2 in an $\Omega = 1$ universe] reveals that all models show a shift toward a network topology if seen with high enough resolution. However, quantitatively the shift is significantly different in different models: the smaller the spectral index n, the stronger the shift. In contrast, the shift toward the *bubble* topology is characteristic only for the $n \leq -1$ models. We find that the mean density of the percolating structures in the nonlinear density distributions generally is very different from the density threshold used to identify them and corresponds much better to a visual impression. We also find that the maximum of the number of structures (connected regions above or below a specified density threshold) in the evolved, nonlinear distributions is always smaller than in Gaussian fields with the same spectrum and is determined by the effective slope at the cutoff frequency.

Subject headings: cosmology: theory — large-scale structure of universe — methods: numerical

1. INTRODUCTION

The topology of the galaxy distribution can provide important clues to the formation of large-scale structure in the universe and the nature of the initial density fluctuations (Shandarin & Zel'dovich 1983). The recent compilation of large galaxy surveys, large in galaxy numbers and survey volumes, has prompted a new round of topological studies of the structure of the universe. The amount of information in studies like the *IRAS* and CfA Redshift Surveys, and the upcoming Sloan Digital Survey suggests that the major problems of discreteness, boundary effects, and local inhomogeneity that have plagued topological analysis to date may be overcome.

Two types of methods have been developed and employed to quantitatively assess the topology of the galaxy distributions of these surveys. The first one is based on the evaluation of the mean Euler characteristic, $\chi(\nu)$, or the genus curve, $g(\nu)$, as functions of the density contrast: $\nu = \delta/\sigma_\delta$ ($g = -\chi/2$) (Doroshkevich 1970; Bardeen et al. 1986; Gott, Melott, & Dickinson 1986).[1] The genus curve method has been utilized for studies of N-body simulations (Gott, Weinberg, & Melott 1987), nonlinear gravitational evolution (Melott, Weinberg, & Gott 1988), and many galaxy catalogs (see, e.g., Weinberg, Gott, & Melott 1987; Gott et al. 1989; Moore et al. 1992; Vogeley et al. 1994).

The other method is based on percolation theory. Percolation is the study of the number and various properties of "clusters."[2] In 1982, Zel'dovich noticed that the percolation properties of the nonlinear density distribution in the hot dark matter (HDM) model are very different from that in the initial Gaussian field. In particular, the formation of a percolating cluster (the cluster spanning through the entire system) happens more effectively than that in Gaussian fields. He also suggested characterizing the topology of nonlinear density distributions by their percolation thresholds (Zel'dovich 1982). Following Zel'dovich's idea, one of the authors of this paper (S. S.) suggested using percolation properties of *the galaxy distribution* as an objective quantitative measure of the topology of the large-scale structure and also as a discriminator between cosmological models (Shandarin 1983; Shandarin & Zel'dovich 1983).

A percolation technique was utilized in the study of the CfA I catalog (Einasto et al. 1984) and showed that the large-scale distribution of galaxies had a network structure. Theoretical studies of models with a power-law initial spectra showed that the $n = -1$ model clearly percolated better than the $n = 0$ model, and in the $\Omega = 1$ universe the $n = -1$ model was in agreement with observations (Gott & Rees 1975; Bhavsar & Barrow 1983). The percolation method also showed that the cold dark matter (CDM) model appeared to have a connected, rather than clumpy, density distribution (Melott et al. 1983; Davis et al. 1985). Later it was pointed out that the major disadvantage of any percolation technique was the dependence of the percolation thresholds on the mean density of the sample (Dekel & West 1985), which made it difficult to calibrate for sparse samples. Similarly, we note that at present some believe that sparse samples can only be reliably used for the estimation of the two-point correlation function (Bouchet 1995). We elaborate on this question below.

For continuous fields such as density fields the independent parameter is the density threshold. A cubic lattice is superimposed on the field, and lattice cells with densities above the threshold are tagged as overdense, while cells below the threshold are labeled underdense. Overdense cells are considered clusters and can merge with other overdense cells to become larger clusters by satisfying a nearest neighbor condition. The nearest neighbor criterion we employ is that overdense cells must share a common side. On a simple cubic lattice, this means that each cell can have up to six

[1] For a general review of this method see, e.g., Melott 1990.

[2] In the absence of a better term, we label as "clusters" the high-density regions bounded by the surfaces of chosen constant density and "voids" as bounded regions of low density. These terms are not to be confused with the astronomical terms, voids and clusters of galaxies.

nearest neighbors.[3] As the value of the threshold density is decreased, more cells will be tagged as overdense and clusters will grow in number and/or size. This process proceeds until the largest cluster spans the available space and percolation is said to have occurred. Void percolation is accomplished in an analogous fashion, except that the density threshold is initially set at a low value and voids grow as the threshold value is increased. To quantify the study of the clusters (voids) formed by the above scheme, we trace the value of the three most robust parameters: the cumulative distribution function, referred to as the filling factor; the volume of the largest structure (cluster or void) as a fraction of the corresponding filling factor; and the total number of all clusters and voids as a function of the filling factor. The rationale for using the filling factor instead of the density contrast as a fundamental parameter is that the filling factor is normalized allowing a direct comparison of the parametric values of Gaussian and nonlinear distributions as well as the topology of overdense and underdense phases. Also, we wish to isolate the information stored in the dependence of the filling factor on the density threshold from that stored in the other statistics.

The percolation threshold of a Gaussian distribution, as described above, is believed to coincide with a change in the sign of the genus; however, there is no theorem proving this. Intuitively, it is plausible that percolation thresholds approximately coincide with changes of the genus sign. Sathyaprakash, Sahni, & Shandarin (1996) showed that in the nonlinear distributions both transitions happen at close but significantly different filling factors.

One advantage of the genus method is the existence of an analytic expression for Gaussian random fields (Doroshkevich 1970; Hamilton, Gott, & Weinberg 1986). Tomita (1986) gave a very elegant analytic expression for the mean Euler characteristic for multidimensional Gaussian fields, and recently an analytic expression was obtained in the weakly nonlinear regime (Matsubara 1994). However, one should not forget that the mean genus is a statistical measure, and therefore an estimate of the dispersion is needed before it becomes meaningful. The dispersion of the genus for finite samples having finite resolution has not been obtained analytically and can be estimated only from numerical simulations. Percolation parameters are also calculated numerically, but if the dispersion can be estimated, the mean can also be estimated with similar accuracy.

It has been claimed that the percolation thresholds are the most sensitive discriminators of varying models (Shandarin 1983). The recent study of the CfA II catalog using the genus method (Vogeley et al. 1994) supports that suggestion. The authors reduced the information of the genus curve to three numbers, one of which was the genus peak width, $W_\nu = \nu_+ - \nu_-$ (where ν_+ and ν_- are the levels at which the genus changes sign). Figures 12–14 in Vogeley et al. (1994) clearly demonstrate that W_ν has the highest discriminating power among three suggested parameters. However, we still believe that the percolation thresholds as well as ν_+ and ν_- should be interpreted separately because they carry independent information about the topology of the structure.

[3] For the versions of percolation analysis utilizing other nearest neighbor definitions or lattice structures; see, e.g., Mo & Börner 1990 and de Lapparent et al. (1991).

The major improvement of the percolation technique we report in this paper is related to the development of an extremely efficient code for finding all the clusters at a given density threshold (Stauffer & Aharony 1992; Klypin & Shandarin 1993). This enables us to calculate more parameters with finer density thresholds variations than in earlier studies. In this paper, we shall report the results of studying the nonlinear density distributions in real space obtained from N-body simulations of the scale-free cosmological models: $P(k) \propto k^n$, with $n = +3, +1, 0, -1$, and -2 in the $\Omega = 1$ universe. The volume of the largest structure will be used in this paper to indicate the onset of percolation and characterize the topology of the distribution. Every generic density distribution at a sufficiently high-density threshold will look like a system of isolated (nonpercolating) clusters. At some lower threshold the connected system spanning through the entire volume will inevitably form. One possible definition of a network distribution would be a distribution for which percolation occurs at a specified density threshold. In this case the choice of the threshold must be physically justified. We do not know how to select this particular density threshold. Therefore, we adopt a different definition of a network distribution. Fields that percolate at lower filling factors than Gaussian fields (by definition structureless) will be interpreted as having a "connected" or network structure; while fields that percolate at higher filling factors will be considered "disconnected" or clumpy. Similarly, we label a distribution as having a bubble topology if the underdense region percolates at a higher filling factor than in a Gaussian field.

It is worth stressing that the terminology in this field is often confusing. We use the labels clumpy, network, and bubble structure to emphasize the degree of connectedness only. In this paper we ignore the geometrical aspect of the problem. For instance, we do not distinguish between a network made of filaments (quasi–one-dimensional objects) or pancakes or sheets (quasi–two-dimensional objects). In realistic distributions, it is often impossible to rationally assign a label to the shape of a particular density enhancement. Various shape statistics (Vishniac 1986; Babul & Starkman 1992; Luo & Vishniac 1995) assume that the shapes can be approximated by a triaxial ellipsoid. However, the dynamics of the nonlinear gravitational evolution suggests that the first collapsed objects (pancakes) have a bowl-like shape (Arnold, Shandarin, & Zel'dovich 1982; Shandarin et al. 1995), which is very poorly approximated by a triaxial ellipsoid. In particular, the thickness of such a structure would be highly exaggerated if it is approximated by an ellipsoid. This problem is addressed in an upcoming paper by Sathyaprakash et al. (1996).

In addition to determining the topology of the density distributions, we will demonstrate a method of estimating the slope of the power spectrum characterizing a distribution. The maximum of the number of clusters (voids) statistic is determined by the effective spectral index at the Nyquist frequency (or the smoothing scale). Potentially, this relation can be used for measuring the slope of the spectrum.

In § 2 we will explain the parameters we use to characterize the density distribution in space and discuss their application to the power-law Gaussian fields. In § 3 we describe the percolation of Gaussian fields, and in § 4 we describe the N-body simulations forming the basis for our standardizations. We detail the results from studying the growth

of the largest structures and elaborate on the number of clusters results in § 5. We summarize our findings in § 6.

2. METHOD

2.1. *Filling Factor*

Percolation theory deals with the number and properties of the clusters. The density threshold δ_c separating overdense ($\delta > \delta_c$) and underdense ($\delta < \delta_c$) regions is assumed to be a free parameter. When analyzing discrete distributions (e.g., galaxy distributions), we assume a smoothing procedure creating a continuous density distribution.

As we mentioned, the density threshold is not a convenient parameter if linear (Gaussian) and nonlinear density distributions or overdense and underdense phases are to be compared. Instead we utilize the filling factor to parameterize the density threshold. In this case one can easily compare the properties of clusters with those of voids and also linear and nonlinear density distributions. In a two-dimensional illustration it would be similar to comparing different patterns, provided that the same amount of paint was used to make each pattern. For reference we provide the relationship between the filling factor and the density contrast, for the models studied (Fig. 1). The effect of evolution on the relationship is evident in the graphs and underscores the reasons to use the filling factor as a means of comparison. One sigma error bars are comparable with or smaller than the thickness of the lines and are not shown. Solid lines and dashed lines show the filling factor for the nonlinear distributions and Gaussian fields with corresponding spectra (see § 2.4).

We study various characteristics of a field as a function of the filling factor, which is the total volume occupied by the regions having a density above (if we study overdense

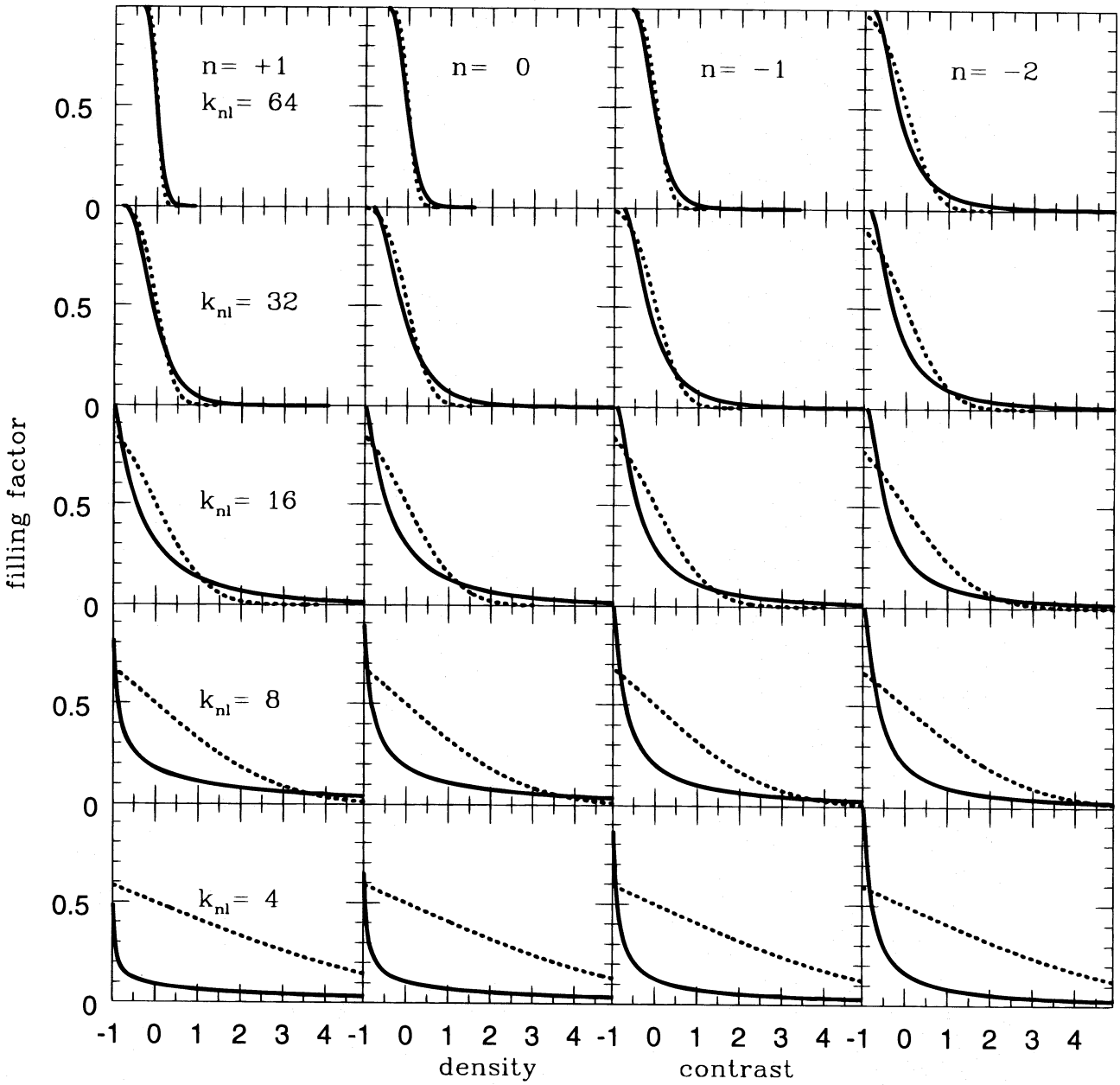

FIG. 1.—Relationship of the cumulative distribution function (filling factor) to the density contrast. Solid lines are distributions derived from *N*-body simulations, and dotted lines are the Gaussian randomizations. One sigma error bars are contained within the width of the lines.

regions) or below (if we study underdense regions) a specified threshold. The filling factor coincides with the "volume fraction" used by Gott, Weinberg, & Melott (1987) in their development of the genus curve for topological analysis and by Vogeley et al. (1994). However, instead of expressing it in terms of ν (the number of standard deviations above or below the mean density of the isodensity contour filling the same volume in a Gaussian field), we use it directly. The filling factor is obviously related to the cumulative distribution function of the corresponding phase:

$$ff(\nu) = \frac{1}{\sqrt{2\pi}} \int_{\nu}^{\infty} e^{-t^2/2}\, dt\ . \qquad (1)$$

Also, in Gaussian fields there is no statistical difference between underdense and overdense regions; therefore, the filling factor is the same for both.

2.2. *Largest Structures*

Here for definiteness we shall talk about overdense regions; the underdense regions can be discussed similarly. For a given density threshold we have a set of regions that differ by volumes, shapes, and other parameters. We select the one having the largest volume and call it the largest cluster. It is convenient to measure the largest cluster and void as a fraction of the corresponding filling factor. Thus, if the largest cluster is 0.9 at a filling factor of 0.2, it means that the density is higher than the chosen threshold in 20% of the volume and almost all of that volume (90%) is comprised of only one connected region. The absolute volume of the largest cluster is clearly 18% of the total volume of the sample.

In a finite system, (like the density distribution in the N-body simulations or galaxy surveys) if we start from a very high-density threshold we do not find any clusters at all. Lowering the threshold we find the first cluster corresponding to the highest density peak. Obviously, it is also the largest cluster, and its volume measured in terms of the filling factor is unity. This is an effect of a finite system and we shall ignore it. In other words, one cannot use the statistics at density thresholds (which are too high) or filling factors (which are too small). At lower thresholds we typically have many clusters. Usually, the volume of the largest cluster is negligible compared to the total volume of all clusters (the filling factor). The actual volume of the largest structure (in the units of the filling factor) can be used as a measure of the fairness of the sample: the smaller the largest structure at low values of the filling factor the better the sample. Decreasing the density threshold we reach the situation where clusters begin to merge. As a result the largest cluster becomes a significant fraction of the filling factor, and eventually almost all overdense regions combine to make just one cluster. At this stage the volume of the largest cluster almost equals the filling factor, and percolation is said to happen. In the past much effort was spent on an accurate measurement of the percolation threshold (Klypin 1987; Dominik & Shandarin 1992; Klypin & Shandarin 1993). In contrast, we use the *largest structure as a function of the filling factor* as a practical indicator of the percolation transition as suggested by Shandarin (1996a,b).

The percolation transition is a universal behavior of every nondegenerate system; however, the filling factor at which the transition happens is particular to each system and may vary. The percolation threshold marks a change in the topology of a distribution. Above the percolation threshold ($\delta_c \geq \delta_p$), the overdense system consists of isolated clusters having finite volumes and the topology is of a meatball or clumpy type (if the underdense regions are considered it is usually called a bubble topology). Below the percolation threshold ($\delta_c \leq \delta_p$), most of the overdense volume is in one cluster spanning the entire system and the topology is labeled a network or sponge topology. Both terms, network topology and sponge topology, correspond to the positive genus, but the term network structure suggests that the percolating structure is "thin," which is a geometrical rather than topological characteristic.

We plot the largest cluster and the largest void volume fractions versus the corresponding filling factor in the same diagram. As we mentioned before, Gaussian fields exhibit no statistical difference between overdense and underdense phases and both structures have similar properties. In contrast, for all nonlinear density distributions the largest cluster percolates as easy or easier (that is at smaller filling factors) than the largest void, which is a manifestation of non-Gaussianity resulting from nonlinear gravitational clustering.

2.3. *Number of Clusters and Voids*

The third type of statistic we use in this paper is the total number of clusters and voids at a given filling factor. The significance of this statistic is its sensitivity to the slope of the spectrum. We shall measure the number of structures per Nyquist volume: $V_{\rm Ny} = \lambda_{\rm Ny}^3 = 8$ mesh cells. The number of clusters and/or voids typically grows with the growth of the filling factor until it reaches the value about 0.1–0.13, then it quickly decreases because of merging of the clusters. In the nonlinear distributions the number of clusters is often (but not always) smaller than that of voids at the same filling factors. Again, the difference between the number of the clusters and voids is a manifestation of non-Gaussianity of the density field.

2.4. *Mixing Phases*

We produce three distinct types of density fields for analysis in this study: random Gaussian fields with pure power-law spectrum, fields derived from N-body simulations with evolved nonlinear power spectrum, and Gaussian fields with nonlinear power spectra produced by randomizing the phases of the N-body simulation distributions. Percolation of Gaussian fields (with linear and nonlinear power spectrum) produces standards for characterizing the topologies and estimating the spectral indices of density fields in subsequent studies. The analysis of fields generated from N-body simulations checks and calibrates our ability to describe fields by the method outlined above.

In the comparison of simulation fields to Gaussian fields, we wish to avoid grid effects as much as possible. Because grid effects are inherent in the method, our solution is to generate nonlinear Gaussian fields from the simulation fields, thereby, assuring grid effects similar to those displayed in the nonlinear, parent distributions. This also resolves the question of how to calibrate the percolation curves for sparse samples. A good way to do this is to start by Fourier transforming a nonlinear N-body simulation field to k-space. Then, in the resulting transform generate random phases keeping the amplitude of every wave exactly the same as before, and finally make an inverse Fourier transform resulting in a new Gaussian field having the same power spectrum as the original nonlinear parent field. We

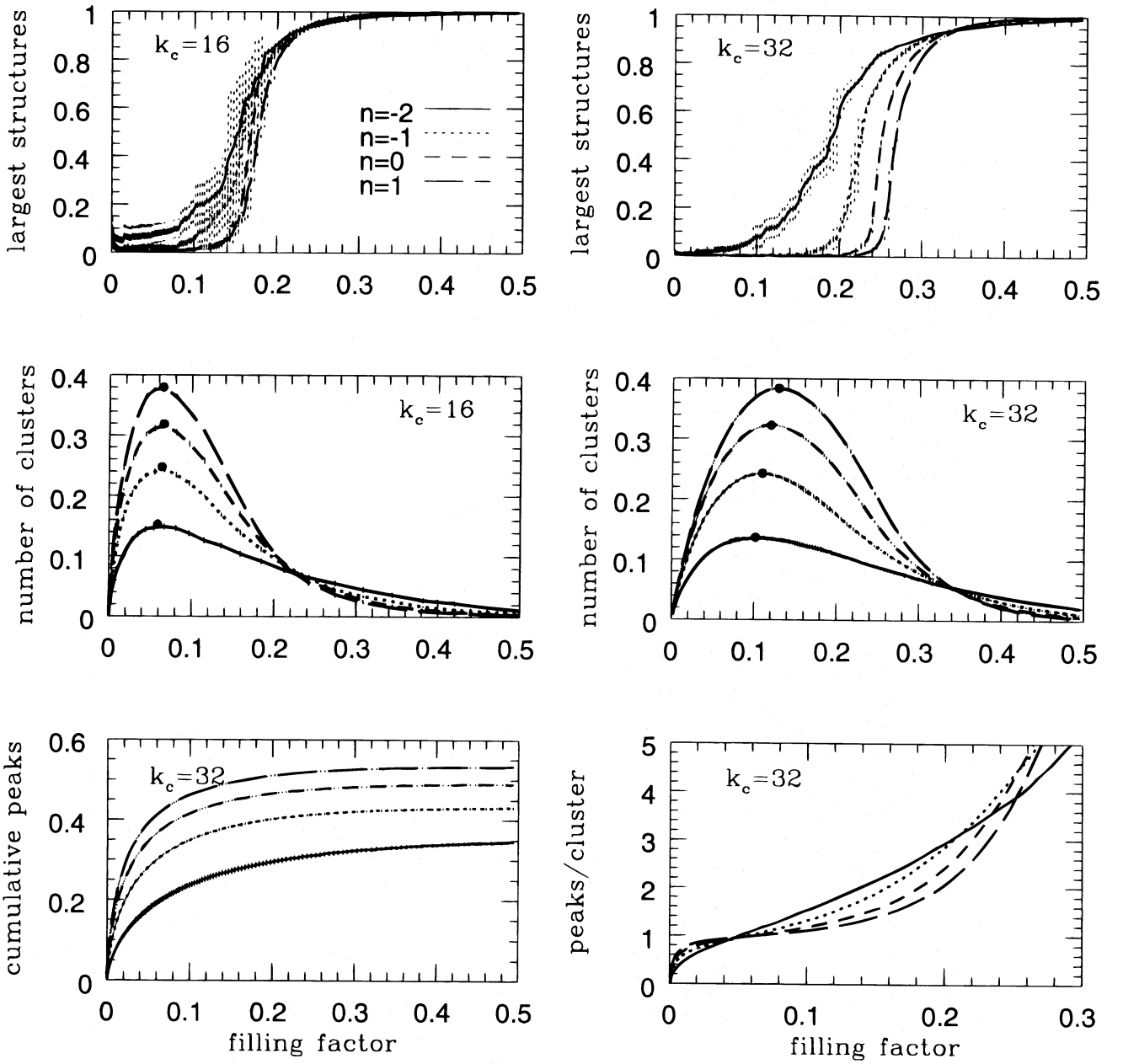

FIG. 2.—Percolation in Grid-Gaussian fields with $k_{cutoff} = 16$ and 32 (where $k_c = 32$ is the Nyquist cutoff). The top panels show the volume of the largest structure in filling factor units. Short dashes display 1 σ dispersion for all graphs. The number of clusters statistic (normalized to the cutoff volume) is shown in the middle panels. Maximum values are marked with dots. The bottom panels display statistics of the density peaks: theoretically calculated cumulative density of peaks (*left*) and the number of peaks to cluster ratio for a given filling factor (*right*).

ignore the fact that this field may have negative values, since we study only the percolation properties parameterized by the filling factor. Since the generated Gaussian field has the same amplitudes, it must be affected by the finite resolution similarly to the nonlinear density fields. This randomized version of the simulation density field is percolated to produce an additional standard for distinguishing the topology of the model and to illustrate the relationship between phase correlations and nonlinearity. The comparison of the nonlinear and randomized (Gaussian) fields provides a measure of the phase correlation in the nonlinear fields. We show and interpret the collective results of the percolation of Gaussian and simulation fields in the following sections.

3. PERCOLATION IN GRID GAUSSIAN FIELDS

The ability to recognize Gaussianity in a distribution is important for two reasons. First random Gaussian fields are used as benchmarks for describing the topology of density fields derived from survey data, and second it has been demonstrated that random phase density fluctuations could be produced by an inflationary period in the early history of the universe (see, e.g., Linde 1990). Importantly, a random Gaussian field is fully distinguished by its associated power spectrum. If gravitational instabilities were the only mechanisms of structure formation and the initial density perturbations were Gaussian, then the initial power spectrum would determine the large-scale structure of the universe.

It is worth emphasizing that random fields generated numerically on a grid are only approximately Gaussian. We shall call them grid Gaussian fields. One obvious deficiency of a grid Gaussian field compared to a true Gaussian field is that the probability distribution function is always wrong for sufficiently large values of the field. We will report another less obvious deficiency related to the topology of the field.

The Gaussian fields we employ in this study are created by transforming an array of coefficients, which are random Gaussian distributed, from k-space to real space. The range of k was limited by both the box size (the fundamental mode, k_f) and the resolution of the mesh (the Nyquist wavenumber, $k_{\rm Ny}$), such that $k_f \le k \le k_{\rm Ny}$. We also study fields with cutoffs for which $P(k) = 0$ for $k > k_c$. The results are Gaussian random density fluctuation fields that are homogeneous and isotropic. These properties insure that the associated power spectrum is a function of k only. The spatial modes of these fields are mutually independent and have random phases. (We exploit this random phase condition of Gaussian fields in our phase mixing of N-body simulations explained above.) It is important to remember that Gaussian fields are by definition structureless.

Figure 2 shows several parameters calculated for grid Gaussian fields with power-law spectra: $P(k) \propto k^n$ with the spectral index $n = -2$, -1, 0, and $+1$. The fields were generated on a 64^3 mesh by Fourier transform of random numbers, so no particles were involved. The results for two cutoff values are shown: $k_c = 16$, and $k_c = 32$ (the Nyquist wavenumber). Four realizations with different random number seeds were generated for each curve, and mean values are plotted. One sigma error bars are also shown, but in some cases they are too small to be seen.

The two top panels show the largest cluster measured as a fraction of the filling factor. The left panel shows the grid Gaussian functions with the power-law spectra cut off at $k_c = 16$, and the right panel shows those without an arbitrary cutoff. According to percolation analysis, percolation in Gaussian fields occurs at $ff \approx 0.16$ (corresponding to $v = 1$) independently of the power spectrum. The onset of percolation is marked by a sharp growth of the largest cluster and corresponds to the change of the topology from meatball to sponge type. The left top panel is in agreement with this result, but the right top panel is not. The right panel shows that the percolation threshold depends on the spectral index; the larger the index, the higher the percolation threshold. Statistically, the difference is highly significant. Thus, the limited resolution of the mesh results in grid Gaussian fields, with no spectral cutoff, having a meatball topology shift indicated by a percolation transition at greater filling factors than true Gaussian fields. This may affect the appearance of the large-scale structure in the N-body simulations especially in those having a small number of particles, making them look more clumpy than they should.

At small filling factors the largest structure must be negligible in sufficiently large samples. The finite size of the largest structure can be used as an internal characteristic of the fairness of a sample. The smaller the largest cluster in the nonpercolating regime the better the sample. One can see that the more negative the spectral index, the more difficult it is to satisfy this condition.

The middle panels show the number of clusters per Nyquist volume (8 mesh cells) as a function of the filling factor. The curves reach their maximum at filling factors of about 0.11 (dependent slightly on the spectral index n) for the spectra with no arbitrary cutoff ($k_c = k_{\rm Ny} = 32$) and drop with the growth of the filling factor because of the merging of clusters. In the $k_c = 16$ models the maxima are reached at filling factors ($ff_{\rm max} = 0.08$) that are roughly half the value of the filling factors at the percolation threshold regardless of the spectral index. The value of the maximum (marked by a dot) depends very weakly on the cutoff and is determined only by the spectral index on the scale of the cutoff. This demonstrates that percolation analysis can discriminate between random Gaussian fields typified by different spectral indices (for pure power-law initial power spectra) as easily as the maximum of the genus curve.

The left bottom panel shows the cumulative number density of peaks calculated analytically using the equation

$$n_{\rm pk}(ff) = \int_{-\infty}^{\nu} N_{\rm pk}(ff)d(ff) \qquad (2)$$

from (Bardeen et al. 1986). Since the statistical properties of Gaussian fields are generally reported in terms of the peaks, an interesting quantity is the number of peaks per cluster, which can be estimated as the ratio of the number of peaks to the number of clusters. This ratio is shown in the lower right panel. For small filling factors ($ff \le 0.02$ or so corresponding to $\nu \ge 2.5$) the number of clusters obtained numerically is unreliable and, therefore, so is the number of peaks per cluster. In the range $0.02 \le ff \le 0.1$ ($1.2 \le \nu \le 2.5$) there is roughly one peak per cluster (however, the exact number depends on the spectral index n). Thus, we conclude that the numerical result is roughly consistent with the analytical calculation of Bardeen et al. (1986). For larger filling factors the number of clusters drops quickly due to merging into the largest cluster and the ratio of the number of peaks to the number of cluster grows limitlessly.

4. N-BODY MODELS

The N-body simulations are produced by a staggered particle-mesh code (Melott 1986) with 128^3 particles on a 128^3 mesh and a corresponding Nyquist wavenumber, $k_{\rm Ny} = 64$. The initial conditions are generated by the Zel'dovich approximation (Klypin & Shandarin 1983) such that the initial power spectrum is a simple power law covering the range $n = 3$, 1, 0, -1, and -2. The models are allowed to evolve gravitationally until nonlinear effects change the slope of the power spectrum. This change indicates that phase correlations have developed between the originally random initial phases.

The extent of nonlinearity can be characterized by the parameter $k_{\rm nl}$, defined by the equation $\sigma_\delta^2 = a^2 \int_0^{k_{\rm nl}} P(k)d^3k = 1$, and in this study we evolve the simulations to values of $k_{\rm nl} = 64$, 32, 16, 8, and 4 (in units of the fundamental frequency). The value of $k_{\rm nl}$ relates to the scale of structure formation in real space. For a detailed discussion of the N-body simulations, see Melott & Shandarin (1993).

Density fields are derived from the above simulations by a cloud in cell method whereby each particle's "weight" is proportionately spread over a 2^3 cell volume and rescaled (8:1) to produce a 64^3 density field. This method implies some smoothing at small scales but reduces shot noise so that further smoothing is not needed before percolation analysis. An ensemble family of four realizations is produc-

ed for each combination of n and k_{nl} to give assessments of the 1 σ level dispersion for each percolation parameter analyzed.

4.1. *Normalization*

It is likely that no single model studied can pretend to explain the real universe. We consider them to be toy models. However, if one wishes to get a rough idea of how they may relate to the real world we provide the following normalizations. We assume that the rms fluctuation in number of galaxies, σ_g, is about unity within spheres of radius 8 h^{-1} Mpc, the rms mass density fluctuation σ_m is parameterized by the "bias factor," b, such that $\sigma_g = b\sigma_m$. We shall assume that $b \approx 1$, which is an adequate assumption for these crude estimates. Melott & Shandarin (1993) showed that for the models in question the scale of nonlinearity measured by the top hat smoothing filter R_{TH} is approximately 2 times greater than k_{nl}^{-1} calculated from the extrapolation of the linear theory (more accurately: $R_{TH} \approx 1.8k_{nl}^{-1}$ in the $n = +1$, 0, and -1 models and $R_{TH} \approx 2.8k_{nl}^{-1}$ in the $n = -2$ model). Thus, identifying every stage with the present time one can roughly estimate the size of a mesh cell: $l_c \approx 25$, 12.6, 6.3, 3.1, and 1.6 h^{-1} Mpc for $k_{nl} = 64$, 32, 16, 8, and 4, respectively. In our models the smoothing has been performed with a top hat filter having a cubic rather than spherical shape, which may add an additional factor $0.6 \approx (4\pi/3)^{-1/3}$ [assuming the volumes of the filters are similar: $l_c^3 = (4\pi/3)(R_{TH}^{(s)})^3$]. Therefore, one can view each stage of the evolution of the models as the density distribution seen after smoothing with a top hat filter of radius $R_{TH}^{(s)} \approx 16$, 8, 4, 2, and 1 h^{-1} Mpc within the volumes of $(64l_c)^3 \approx (1600\ h^{-1}\ \mathrm{Mpc})^3$, $(800\ h^{-1}\ \mathrm{Mpc})^3$, $(400\ h^{-1}\ \mathrm{Mpc})^3$, $(200\ h^{-1}\ \mathrm{Mpc})^3$, and $(100\ h^{-1}\ \mathrm{Mpc})^3$ for $k_{nl} = 64$, 32, 16, 8, and 4, respectively. The purpose of these estimates is to give a rough idea of the range of parameters characterizing the models, and therefore more elaborate calculations are probably not needed.

5. NONLINEAR GRAVITATIONAL DISTRIBUTIONS

5.1. *Largest Cluster and Largest Void*

Figure 3 shows the largest cluster and largest void statistic for families of four N-body models covering the complete range of initial power spectra taken at all five stages of the evolution. Each panel shows three curves: the largest cluster and void in the N-body simulation, and the largest structure in the Gaussian field having identical Fourier amplitudes with the N-body simulation. Again, in Gaussian fields there is no statistical difference between the largest cluster and largest void because of the symmetry of the distribution.

In Gaussian fields the percolation transition happens at a filling factor of about 16% corresponding to $\nu = \pm 1$. However, the finite size and resolution of the sample biases the transition. In order to avoid these effects, we obtain the "Gaussian" distribution by mixing the phases as described before. This allows for the generation of as many Gaussian realizations with identical amplitudes as needed to estimate the dispersion. The Gaussian, largest structure is shown as a dotted line in Figure 3 (hidden by the shade of the error bars) usually lying between the solid and dashed lines.

The $n = +1$ model demonstrates the smallest difference between the properties of the largest cluster and largest void. Both percolate slightly, yet significantly, better than the corresponding Gaussian field. The $n = 0$ model shows that the underdense regions percolate similarly to the corresponding Gaussian field, but the overdense regions percolate better than the corresponding Gaussian field. These models exhibit a network topology for both clusters and voids. In the $n = +3$ model (not shown) the underdense phase consistently percolates easier than the overdense phase, and the overdense phase percolates similarly to the Gaussian field except that it percolates easier in the last evolutionary stage ($k_{nl} = 4$).

The major feature of the nonlinear distribution is that the largest cluster percolates easier than in the Gaussian case. The significance of this conclusion for the largest cluster is at the many-sigma level for most of the patterns. Qualitatively, this remains true for other models we have studied earlier (CDM, C+HDM; Klypin & Shandarin 1993), but quantitatively the transitions are different. The overdense regions form a connected network spanning through the whole region when the filling factor is relatively small (smaller than in the Gaussian case), and this transition can be labeled as a shift toward a network structure. On the contrary, the underdense regions may not always form a percolating void until the filling factor of the low-density phase is significantly greater than that in the Gaussian field. This type of transition can be labeled as a shift toward a bubble structure. The range of the filling factor corresponding to a sponge topology is typically (but not necessarily) increased compared to the Gaussian case. Thus, the above changes can also be labeled as a shift to a sponge topology. Results (not shown) from the percolation of the $n = 3$ models demonstrate a smooth transition from a connected topology for both clusters and voids to the bubble topology of the $n = -2$ models. In addition, the $n = 3$ case supports our claim of the universality of a filamentary nature for the mass distributions. However, the major point is not how to label a structure but rather to show that in a general case the two shifts are independent of each other and carry independent information about the structure. Therefore, combining them into one parameter (like $W_\nu = \nu_+ - \nu_-$ mentioned above) results in the loss of information. Similar to Gaussian fields at small filling factors, the largest structure must be negligible in sufficiently large samples to insure a fair sample.

5.2. *Density Contrast of the Largest Cluster*

The significance of the percolation transition in the nonlinear gravitational distributions sometimes is challenged on the grounds of the low-density threshold of the percolation onset. However, these numbers may be misleading. We believe that the mean density is more relevant. Let us imagine that we have two identical density contours with $\delta = 0.5$ in two dimensions. Within one of them there are a few peaks the highest of which is $\delta \approx 1$ and within the other one there are few peaks of order $\delta \approx 10$. Now the question is which of these two contours will be picked up by the eye? We believe that obviously the latter is more noticeable. In the linear regime both the mean density and the density threshold are close, but in the nonlinear regime they are very different. Figure 4 shows the mean density of the largest cluster as a function of its volume given in units of the filling factor. For comparison, the density contrast is plotted as a thin line and is markedly below the mean density in every case. An interesting feature of this figure is the stability of the mean density of the largest cluster

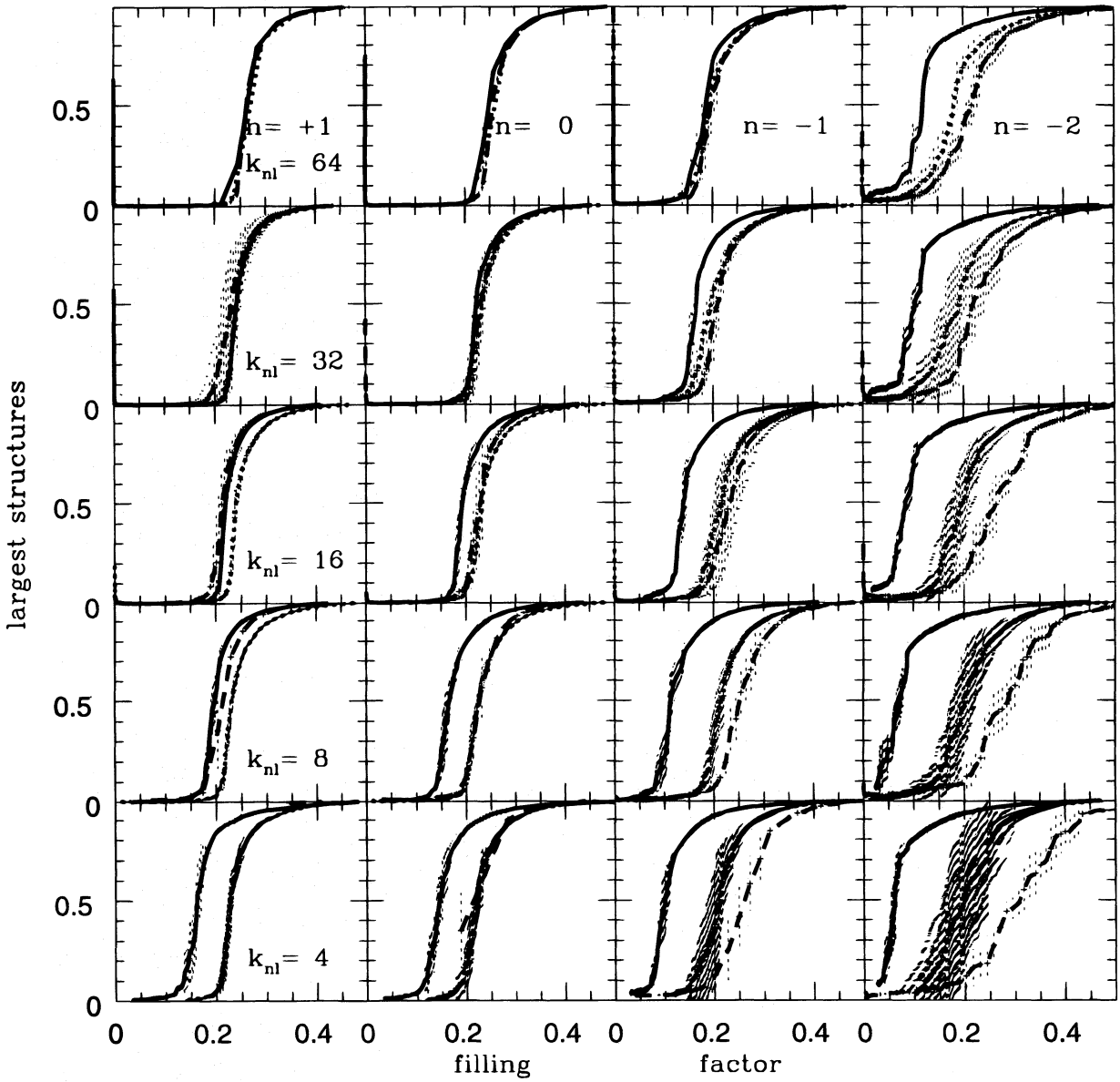

FIG. 3.—Percolation of nonlinear density fields derived from N-body simulations and the Gaussian randomizations. Cluster (overdense) percolation is shown by solid lines, void (underdense) percolation by dashed lines, and dots represent the percolation of the randomized fields. The volumes of the largest structures are plotted in units of the filling factor. Short dashes reflect dispersion at the 1 σ level.

through the percolation transition. The other important aspect of the figure is the value of the mean density at percolation. At percolation the mean density of the largest cluster is well above the average density of the distributions and understandably increases with evolution and decreasing spectral index. The double-valued nature of the function for the early stages of some models is an effect of a finite system explained above (§ 2.2).

5.3. *Number of Clusters and Voids*

Another statistic characterizing the density distribution is the total number of clusters and voids as a function of the filling factor. As mentioned before this statistic is sensitive to the slope of the spectrum in the Gaussian fields. The number of clusters and voids is normalized to the Nyquist volume (8 mesh cells) as was done for Gaussian distributions. Frequency distribution studies establish that the smallest structures (both clusters and voids) dominate in the total number of structures for all spectra studied. Figure 5 shows this statistic for all models and all stages (except $n = 3$). Three curves are plotted for each pattern. The total number of clusters and the total number of voids in the nonlinear distributions, and the total number of clusters (or voids) in corresponding Gaussian fields after randomization of phases. Typically, the number of both clusters and voids in the parent N-body simulation is less than that in the corresponding nonlinear Gaussian field. Thus, the phase correlation due to nonlinear gravitational effects reduces the number of both overdense and underdense structures. The smaller the spectral index, n, the stronger the effect. The number of voids is consistently greater than the number of clusters in the nonlinear distributions if $n \leq 0$. On the other

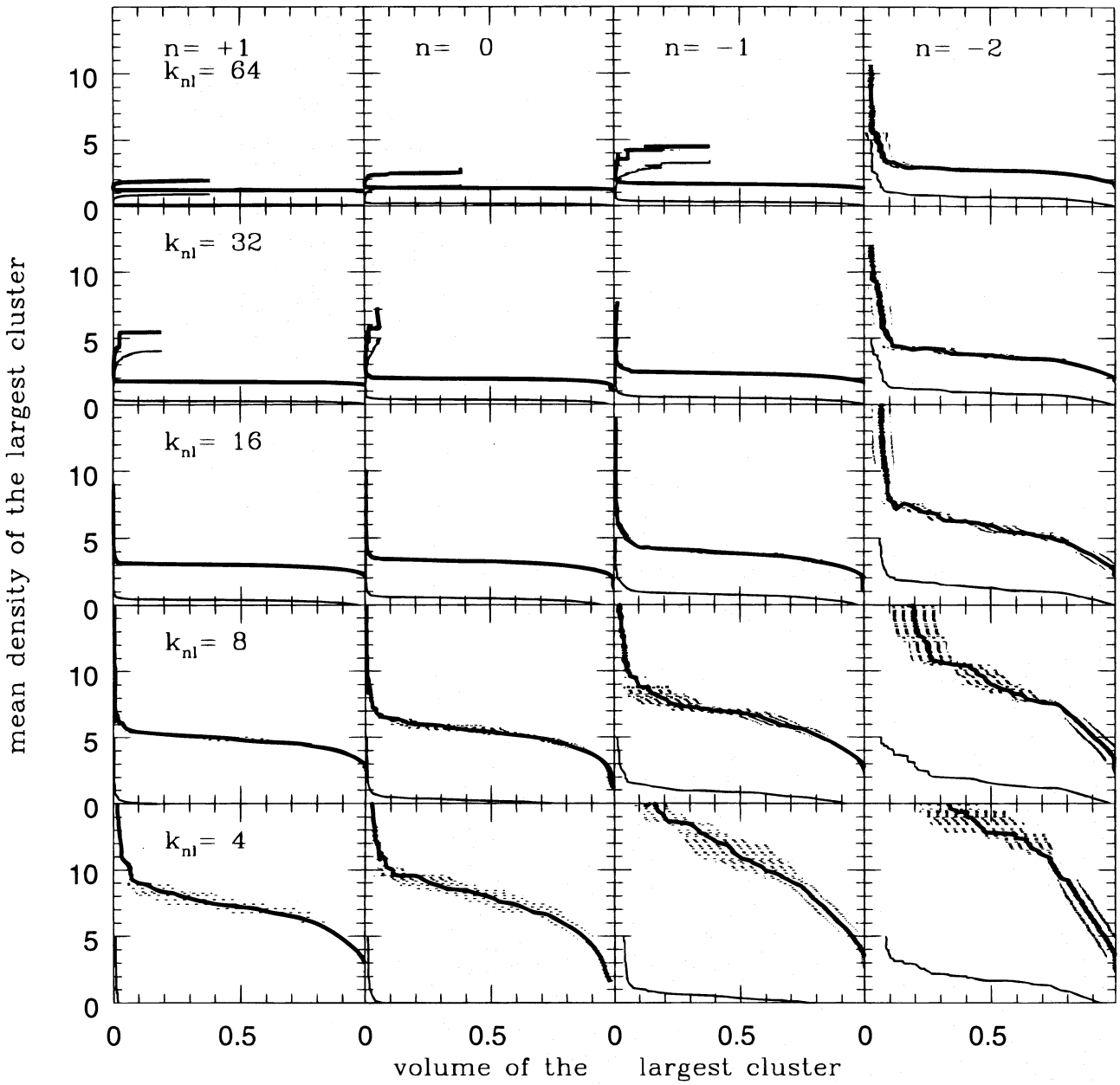

FIG. 4.—Mean densities of the largest cluster produced in N-body simulations compared to the normalized volumes. Where visible small dashes represent 1 σ dispersions. The thin lines are the value of the density contrast supplied for comparison.

hand, the number of clusters is greater in the $n = +1$ model.[4] Another important trend is that at the later stages the differences between models become weaker compared to the beginning stages. With evolution, the models tend toward an estimated slope of $n \approx -1$ in the nonlinear regime, which is in very good agreement with the direct measurement of the spectra (Melott & Shandarin 1993).

Using the right middle panel of Figure 2 as a calibration, one can estimate the slope of the spectra for the nonlinear distributions by extrapolating between the maximum values from the pure power-law Gaussian fields. The maximum values from both types of Gaussian fields are arranged in Table 1 with the estimated slopes in parentheses. Although the table is generally consistent with the trends described above, two anomalies are apparent in the results. First, the maximum value for the case $n = -1$, $k_{nl} = 64$ is considerably below the corresponding Gaussian value; second, the models $n = -1$ and $n = -2$ do not monotonically approach a limiting slope of -1. Both of these peculiarities have a single explanation. Close inspection of the evolved power spectra for these models (see Melott & Shandarin 1993) shows that the same conditions apply to the slopes of the power spectrum if measured at $k = 32$. The Nyquist frequency of the Fourier transform used to produce the nonlinear Gaussian fields is $k_{Nq} = 32$. This suggests that our randomization procedure is sensitive to the slope of the

[4] The last two stages ($k_{nl} = 8$ and 4) in the $n = +1$ model and the very last stage ($k_{nl} = 4$) in the $n = 0$ model suffer from discreteness. The voids are completely empty and percolate at such low-density thresholds that the onset of percolation cannot be reliably calculated in the N-body simulations in question.

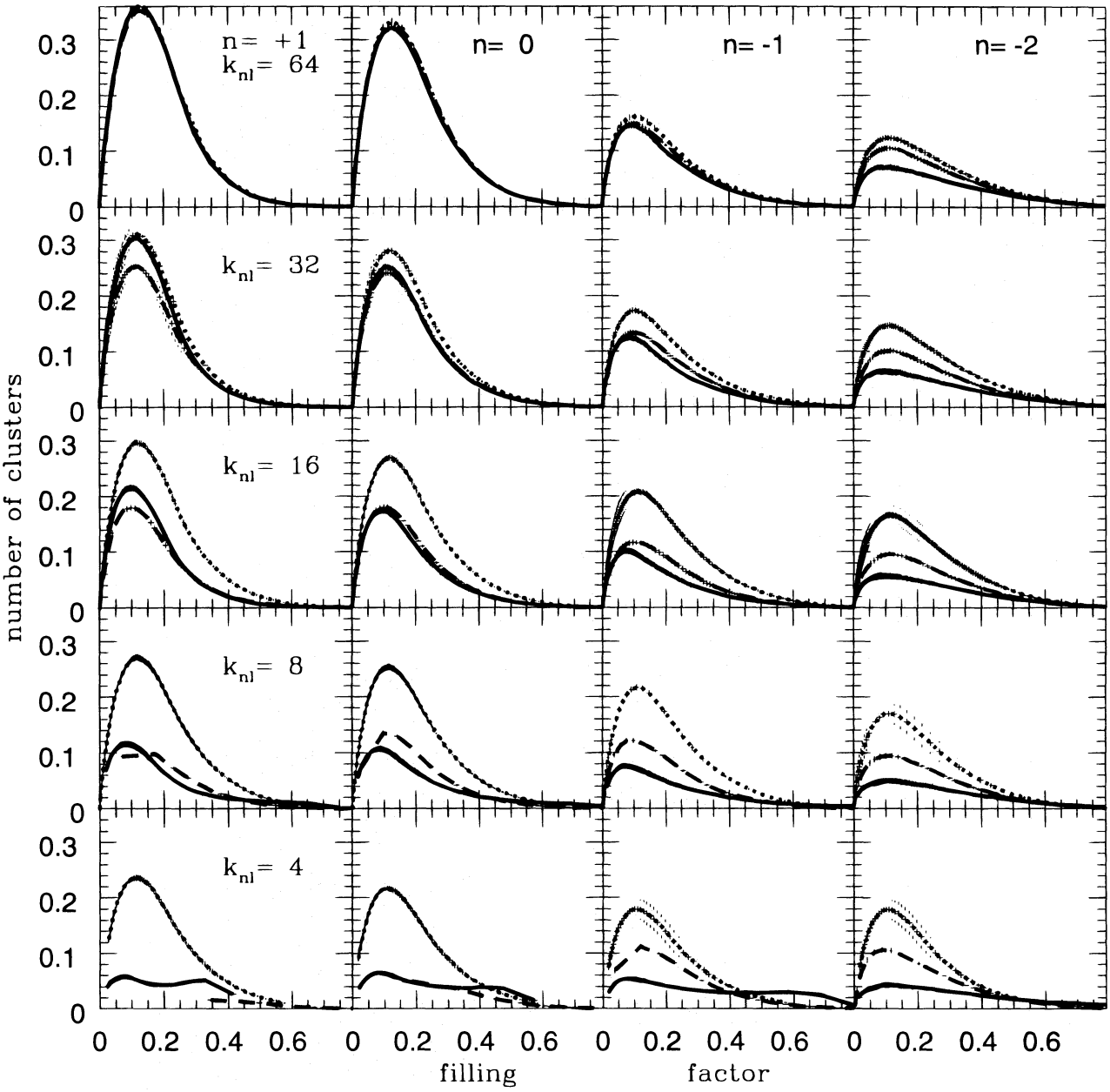

FIG. 5.—Number of clusters per Nyquist volume (λ_{Ny}^3) for a given filling factor. Solid lines are statistics for clusters, dashed lines for voids, and dots for Gaussian randomizations. Short dashes represent 1 σ level dispersions.

power spectrum of the parent field at the maximum value of k used in the Fourier transform. In these cases, the density fields were 64^3 fields with maximum k-values equal to the Nyquist wavenumber, but other cutoff values, $k_c \leq k_{Nq}$, could be enforced. Further study is needed to make the dependence of the slope on the cutoff (k_c) of the randomization procedure a practical technique to measure the effective slope of spectra. The models $n = 1$ and $n = 0$ do not exhibit the anomalies explained above because their power spectra correspond to the trends at the Nyquist frequency.

TABLE 1

NUMBER OF CLUSTERS MAXIMA (ESTIMATED SLOPES)

		N-BODY SIMULATIONS				
n	GAUSSIAN	$k_{nl} = 64$	$k_{nl} = 32$	$k_{nl} = 16$	$k_{nl} = 8$	$k_{nl} = 4$
1	0.38[a]	0.37 (0.4)[b]	0.31 (−0.2)	0.30 (−0.4)	0.27 (−0.7)	0.24 (−1.1)
0	0.32	0.33 (0.1)	0.28 (−0.6)	0.27 (−0.7)	0.25 (−0.9)	0.22 (−1.2)
−1.....	0.24	0.16 (−1.8)	0.17 (−1.7)	0.21 (−1.3)	0.22 (−1.3)	0.18 (−1.6)
−2.....	0.14	0.12 (−2.2)	0.15 (−1.9)	0.17 (−1.8)	0.18 (−1.7)	0.15 (−1.9)

[a] Maxima have errors of ±10%.
[b] Estimated slopes are reported in significant figures.

6. DISCUSSION

The quantitative topology proved to be a useful measure for studying the large-scale structure in the universe. We use a percolation technique to study the mass distribution in real space obtained from N-body simulations of power-law initial spectra: $P(k) \propto k^n$ with $n = +3, +1, 0, -1$, and -2 in the $\Omega = 1$ universe. Five stages corresponding to the scale of nonlinearity at $k_{nl} = 64$, 32, 16, 8, and 4 are analyzed. Each model was run with four different sets of random numbers to create ensemble families so that the dispersion of statistical parameters could be estimated.

We discuss in detail only two robust characteristics calculated in percolation analysis: (1) the normalized volume of the largest cluster (or void), and (2) the total number of clusters (or voids) as a function of the filling factor. It is important to stress that the statistical properties of clusters and voids are identical in Gaussian fields, but they are significantly different in the nonlinear distributions drawn from the N-body simulations. Thus, both statistics are sensitive to the non-Gaussianity of a field. These two functions can be very efficient discriminators of the models. All of the density distributions studied here have unique sets of the three functions (the filling factor, the largest structures, and the number of structures) on a multi-sigma level.

Combining the results that the most numerous clusters are the size of the cutoff scale, and that the nonlinear distributions percolate better than the Gaussian fields, we conclude that the small clusters are arranged in accordance with an underlying network structure. A similar conclusion was derived from the adhesion approximation (Kofman et al. 1992), and the truncated Zel'dovich approximation (Coles, Melott, & Shandarin 1993; Pauls & Melott 1995). The largest cluster as well as the largest void statistics indicate the percolation thresholds, which are associated with a change in the topology of the distributions. The onset of percolation in the overdense phase marks the transformation from a clumpy (meatball) to a network (sponge) topology, and the onset of percolation in the underdense phase marks the transition from a bubble to a network topology. Comparing the simulations with the Gaussian fields we conclude:

1. For all models with $n \leq +3$ overdense regions percolate better than the corresponding Gaussian fields showing a shift toward a network structure. The later the stage, the more significant the shift. Since the models are approximately scale-free, the later stages can also be interpreted as earlier stages of the same distribution seen with better resolution. Thus, we conclude that all power-law models with $n \leq +3$ show a network structure in the density distribution at the nonlinear stage if seen with sufficient resolution. Any differences are only quantitative, but highly significant. The smaller the spectral index the stronger the shift. From this, we conclude that all realistic cosmological models (with non–power-law, initial spectra like the CDM family) can be characterized as filamentary or network structures as far as the mass density in real space is concerned. At early stages of the CDM or C+HDM models when the effective slope at the scale of nonlinearity is small enough ($n_{eff} < -1$), the density distribution is also of a bubble type.

2. The percolation transition happens at relatively low-density contrasts. The larger the value of n, the smaller the density contrast at the percolation threshold (compare Figs. 3 and 4). However, the density threshold is a misleading parameter. We propose the mean density of the largest cluster to characterize the prominence of the transition. The value of the mean density of the largest structure at the percolation transition indicates a definite nonlinear character for the largest cluster.

3. Underdense regions percolate at lower filling factors than their Gaussian counterparts for $n = +3$ and $+1$, and at considerably higher filling factors for $n = -2$. There is a smooth and consistent trend for underdense regions to percolate with greater difficulty as the spectral index decreases or with evolution of a simulation. This trend represents a shift toward a bubble topology for models with $n \leq -1$ indicated by the underdense regions percolating at higher filling factor values than the corresponding Gaussian fields, while the overdense regions percolate at lower filling factors than the corresponding Gaussian fields. There is a noteworthy quantitative difference between the models $n = -1$ and $n = -2$.

4. If the density threshold is selected so that the overdense and underdense phases each occupy 50% of the volume, then all models show that the largest cluster and void occupy almost all of the space. All smaller structures combined occupy at most a few percent of the volume for all the power-law models studied. Thus, the distribution can be labeled as a sponge topology as predicted by Gott, Melott, & Dickinson (1986). Table 2 gives the fractions of the total volume for all clusters and voids (except the largest structures) when the filling factor is 0.5, and the corresponding values for the Gaussian fields. Despite the smallness of the numbers they are highly significant. This explains why Weinberg, Gott, & Melott (1987) found that the nature of the interlocking, equal-volume, overdense, and underdense regions of a random field was a "sponge topology" where both the underdense and overdense regions are equivalent.

5. Our results show that all approximations for a nonlinear, gravitational instability based on nonlinear transformations of initial Gaussian density fields (e.g., the lognormal model) make incorrect predictions of the topology, since they preserve the similarity in percolation properties of the

TABLE 2

VOLUME FRACTIONS IN CLUSTERS/VOIDS/GAUSS (EXCEPT THE LARGEST STRUCTURE)

	k_{nl}				
INDEX	64	32	16	8	4
$n = 0$	0.8/0.8/0.2[a]	0.6/0.6/0.2	0.4/0.4/0.2	0.4/0.4/0.2	1.4/0.5/0.2
$n = -1$.....	0.8/0.8/0.5	0.5/0.6/0.5	0.5/0.7/0.5	0.4/0.8/0.4	1.0/1.0/0.5
$n = -2$.....	0.8/1.7/0.8	0.9/2.0/1.0	0.6/2.2/1.0	0.6/2.7/1.0	0.8/5.0/1.0

[a] All fractions reported in percent (at a filling factor of 0.5). Values displayed are significant figures.

overdense and underdense phases to that of the Gaussian fields.

We acknowledge the support of NSF grant AST-9021414, NASA grant NAGW-3832 and the University of Kansas GRF-95 grant. We thank Adrian Melott for discussions and for supplying the simulations, which were all produced at the National Center for Supercomputing Applications. We also thank L. Kofman, V. Sahni, and B. Sathyaprakash for discussions and comments.

REFERENCES

Arnold, V. I., Shandarin, S. F., & Zel'dovich, Ya. B. 1982, Geophys. Astrophys. Fluid Dyn., 20, 111
Babul, A., & Starkman, G. D. 1992, ApJ, 401, 28
Bardeen, J. M., Bond, J. R., Kaiser, N., & Szalay, A. S. 1986, ApJ, 304, 15
Bhavsar, S., & Barrow, J. 1983, MNRAS, 205, 61
Bouchet, F. 1995, unpublished
Coles, P., Melott, A. L., & Shandarin, S. F. 1993, MNRAS, 260, 572
Davis, M., Efstathiou, G., Frenk, C., & White, S. D. M. 1985, ApJ, 292, 371
de Lapparent, V., Geller, M., & Huchra, J. P. 1991, ApJ, 369, 273
Dekel, A., & West, M. J. 1985, ApJ, 288, 411
Dominik, K., & Shandarin, S. F. 1992, ApJ, 393, 450
Doroshkevich, A. G. 1970, Astrophysics, 6, 320
Einasto, J., Klypin, A. A., Saar, E., & Shandarin, S. F. 1984, MNRAS, 206, 529
Gott, J. R., Melott, A. L., & Dickinson, M. 1986, ApJ, 306, 341
Gott, J. R., et al. 1989, ApJ, 340, 625
Gott, J. R., & Rees, M. J. 1975, A&A, 45, 365
Gott, J. R., Weinberg, D. H., & Melott, A. L. 1987, ApJ, 319, 1
Hamilton, A. J. S., Gott, J. R., & Weinberg, D. 1986, ApJ, 309, 1
Klypin, A. A. 1987, Soviet Astron., 31, 8
Klypin, A. A., & Shandarin, S. F. 1983, MNRAS, 20, 891
———. 1993, ApJ, 413, 48
Kofman, L., Pogosyan, D., Shandarin, S. F., & Melott, A. L. 1992, ApJ, 393, 437
Linde, A. D. 1990, Particle Physics and Inflationary Cosmology (New York: Harwood)
Luo, S., & Vishniac, E. 1995, ApJS, 96, 429
Matsubara, T. 1994, ApJ, 434, L43
Melott, A. L. 1986, Phys. Rev. Lett., 56, 1992
Melott, A. L. 1990, Phys. Rep., 193, 1
Melott, A. L., Einasto, J., Saar, E., Suisalu, I., Klypin, A. A., & Shandarin, S. F. 1983, Phys. Rev. Lett., 51, 935
Melott, A. L., & Shandarin, S. F. 1993, ApJ, 410, 469
Melott, A. L., Weinberg, D. H., & Gott, J. R. 1988, ApJ, 328, 50
Mo, H. J., & Börner, G. 1990, A&A, 238, 3
Moore, B., et al. 1992, MNRAS, 256, 477
Pauls, J. L., & Melott, A. L. 1995, MNRAS, 274, 99
Sathyaprakash, B., Sahni, V., & Shandarin, S. F. 1996, MNRAS, in press
Shandarin, S. F. 1983, Soviet Astron. Lett., 9, 104
———. 1996a, in Proc. Workshop on Large-Scale Structure in the Universe: Theoretical and Observational Aspects, ed. J. Mücket (Singapore: World Scientific), in press
———. 1996b, in Proc. 15th Moriond Astrophysics Meeting on Clustering in the Universe, ed. C. Balkowski, S. Maurogordato & J. Trân Thanh Vân (Gif-sur-Yvette: Editions Frontières), in press
Shandarin, S. F., & Zel'dovich, Ya. B. 1983, Comm. Astrophys., 10, 33
Shandarin, S. F., Melott, A. L., McDavitt, K., Pauls, J. L., & Tinker, J. 1995, Phys. Rev. Lett., 75, 7
Stauffer, D., & Aharony, A. 1992, Introduction to Percolation Theory (London: Taylor & Francis)
Tomita, H. 1986, Prog. Theor. Phys., 76, 952
Vishniac, E. 1986, in Inner Space/Outer Space, ed. E. W. Kolb et al. (Chicago: Univ.Chicago Press), 190
Vogeley, M. S., Park, C., Geller, M. J., Huchra, J. P., & Gott, J.R. 1994, ApJ, 420, 525
Weinberg, D. H., Gott, J. R., & Melott, A. L. 1987, ApJ, 321, 2
Zel'dovich, Ya. B. 1982, Soviet Astron. Lett., 8, 102